Supporting Information

Discovery of a Non-Classic Host Guest Complexation Mode in a β-Cyclodextrin/Propionic Acid Model

Roi Rutenberg,[b,a] Gregory Leitus,[c] Elazar Fallik,[a] and Elena Poverenov[a]*

[a]Postharvest and Food Sciences, Agricultural Research Organization, The Volcani Center, Bet Dagan 50250, Israel
[b]Institute of Biochemistry, Food Science and Nutrition, Faculty of Agriculture, Food and Environment, The Hebrew University of Jerusalem, Rehovot 76100, Israel
[c]Department of Chemical Research Support, Faculty of Chemistry, Weizmann Institute of Science, Rehovot 76100, Israel

* Author for correspondence elenap@volcani.agri.gov.il

Experimental Methods	S2
Spectroscopic Data	S5
Thermodynamic Data	S7
Crystallographic Data	S9
Computational Data	S14
References	S21

Experimental Methods

Materials PA (99%) was purchased from Alfa Aesar (Heysham, England). *β*-CD was purchased from Chem-Impex Int'l Inc. (Wood Dale, IL, USA). D_2O (99.9%) was purchased from Merck. All regents and solvents were used without further purification.

Spectral methods All NMR samples were prepared at 15 mM using D_2O. These included 3 solutions of the host (*β*-CD), guest (PA), and a host and guest (*β*-CD-PA) mixture at a 1:1 ratio. ^{1}H-NMR and diffusion experiments were performed on a 500 MHz Avance III Bruker (Karlsruhe, Germany) NMR spectrometer equipped with a pulsed gradient unit capable of producing magnetic field pulse gradients of about 50 G cm^{-1} in the z-direction. The experiments were carried out using a 5 mm BBFO probe. The pulse gradient separation was 50 ms. The pulsed gradients were incremented from 0 to 30 G cm^{-1} in 10 steps, and their duration in all experiments was 4 ms. Experiments were performed in triplicates at 296º K. ^{13}C-NMR was carried out on a 100.6 MHz instrument. Chemical shifts are reported in parts per million (ppm). ^{1}H-NMR spectra were calibrated to HOD (4.83 ppm). FTIR spectra were recorded between 400 and 4000 cm^{-1} by averaging 100 scans with a 4 cm^{-1} resolution (Bruker Tensor 27 FTIR Spectrometer) using KBr discs.

Determination of binding constant The association constant was determined by evaluating the changes in the diffusion coefficients of the guest upon addition of the host. The diffusion coefficients were determined by the LED technique according to which the ratio between the echo intensity in the presence (I) and in the absence of pulsed gradient (I_0) is given by equation 1 in which γ is the magneticgyro ratio, g is the pulsed gradient strength, Δ and δ are the time separation between the pulsed-gradients and their duration, respectively, and D is the diffusion coefficient.[1] For an isotropic solution, a plot of $ln(I/I_0)$ vs. b should give a straight line, whose slope is equal to $-D$.

(1) $$\ln(I/I_0) = -\gamma^2 g^2 \delta^2 (\Delta - \delta/3) D = -bD$$

From the changes in the diffusion coefficients of the guest upon addition of the host, the bound fractions were calculated and then translated to an association constant K_a as described previously[2] and then to ΔG.[3] Thermodynamic parameters in the spectral section were calculated utilizing diffusion NMR measurements.[4]

Thermodynamic methods Thermodynamic parameters were obtained using a method previously published.[5] Shortly, a *β*-CD-PA (88 mM : 15 mM, respectively) aqueous solution in DDW (doubly diluted water) was stirred and heated from 311º K to 326º K, while measuring its shift in pH values. pH and temperature measurements were taken using an EC-150 pH-Temp meter from Phoenix instruments (Garbsen, Germany). Changes in pH indicated the degree of PA dissociation after subtracting the [H^+] donations from *β*-CD and DDW. Change of PA's pKa values in different temperatures was taken into account,[6] as well as *β*-CD's complexation ability in different pH environments.[7] K_a was thusly calculated and applied linearly to Van't Hoff plots to extract thermodynamic parameters according to the Van't Hoff equation (equation 2).

(2) $$R \ln K_a = \frac{-\Delta H}{T} + \Delta S$$

Computational methods Docking; Multi-step docking protocol was employed as described. First, ~10,000 docking positions around a geometric center of a *β*-CD molecule were generated for each guest molecule by using a genetic algorithm. Both host (*β*-CD) and guests (neutral and anionic forms of PA) were kept rigid ("rigid-body" approximation). Initial search was performed within the sphere of a ~11 Å diameter. Then, all degrees of freedom were released. Each "rigid-body" docking configuration was refined by using "grasp" (torsion space optimizer) and "trunc" (truncated Newton method minimizer) algorithms as implemented in the AMMP set of programs.[8] Each pose was evaluated based on the computed host-guest interaction energy. Therefore, both "host" and "guests" were finally treated as flexible molecules.

Molecular dynamics (MD) simulations. The all-atom MD simulations were performed using the GROMACS 4.5.5 program package.[9,10] All-atom topology parameters, AM1-optimized geometry and MOPAC charges for *β*-CD (1), PA in an ionized carboxylate form (2), and neutral/uncharged PA (3) were generated using the Automated Topology Builder (ATB).[11] Water molecules were modeled as single point charges (SPCs), and the GROMOS force field 53a6 was applied to 1, 2, and 3. To simulate the interaction of *β*-CD with two forms of PA, two starting configurations (1-2 and 1-3) obtained from the docking study (as described in above) were taken. Each system (1-2 and 1-3) was placed in a 5×5×5 nm^3 box. The box was solvated by 3343 water molecules treated as SPCs. Sodium counter ion was then added to the 1-2 system, to make it electrically neutral (zero net charge). The energy of each system was minimized by using the steepest descent method followed by conjugate gradient minimization. To relax water molecules, 100 ps MD simulations were subsequently performed at constant volume and temperature (300 *K*), and the positions of all non-hydrogen atoms were restrained by force constants of 1000, 500, 250, and 100 $kJmol^{-1}Å^{-1}$ to achieve a better relaxation for initial configuration. To restrain bond lengths, the LINCS algorithm[12] was applied with a 2 fs integration step, and the neighbor list for calculation of non-bonded interactions was updated every five time steps. Periodic boundary conditions were used, and electrostatic interactions were calculated by using the PME method[13,14] with a short-range cutoff of 1 nm. For the Lennard-Jones interactions, a cutoff value of 1 nm was used. In the production simulations, the final unrestrained 50 ns trajectories were generated at a constant pressure of 1 bar and a temperature of 300º K using the Berendsen thermal bath and pressure coupling.[15]

Crystallographic methods The *β*-CD-PA IC colorless crystals (elongated plates) suitable for a single crystal X-ray analysis were obtained by recrystallization from a 323º K 5 mL aqueous solution of *β*-CD-PA (0.03:1.2 M) to 284º K. *Crystal data:* empirical formula: $C_{45}H_{90}O_{49.63}$ ($C_{42}H_{70}O_{35}$+$C_3H_6O_2$+12.63*(H_2O)), 0.18 x 0.15 x 0.06 mm^3, Monoclinic, $P2_1$, a=15.517(3) Å, b=9.825(2) Å, c=21.953(4) Å, *β*=90.05(3)º from 20 degrees of data, T=100(2) K, V=3346.8(11) $Å^3$, Z=2, Fw=1425.25 g/mol, Dc=1.414 $Mg.m^{-3}$, μ=0.131 mm^{-1}. *Data collection and processing:* Bruker Appex2 KappaCCD diffractometer, MoKα (λ=0.71073Å), graphite monochromator, 35176 reflections collected, -18≤h≤18, -11≤k≤11, -26≤l≤24, frame scan width = 0.5°, scan speed 1° per 300 sec, typical peak mosaicity 0.67°, 12407 independent reflections (R-int=0.0821). The data were processed with Bruker Appex2 software. *Solution and refinement:* Structure solved by

direct methods with ShelexT. Full matrix least-squares refinement based on F^2 with ShelxL. 996 parameters with 59 restraints, final R_1= 0.0680 (based on F^2) for data with $I>2\sigma(I)$ and, R_1= 0.0741 on 12407 reflections, goodness-of-fit on F^2 = 1.064, largest electron density peak = 0.724 $Å^{-3}$, deepest hole -0.445 $Å^{-3}$.

Spectroscopic Data

Table S1 ^{1}H and ^{13}C chemical shifts corresponding to PA and *β*-CD in their free form (δ_0) and *β*-CD-PA IC form (δ) [ppm]. The shift displacement (Δδ) was calculated according to $\delta-\delta_0$.

^{1}H #	δ_0	δ	Δδ	^{13}C #	δ_0	δ	Δδ
PA				PA			
CH_3-	1.1299	1.1354	0.0055	**C**H_3-	8.2853	8.4249	0.1396
-C**H_2**-	2.4319	2.4310	-0.0009	-**C**H_2-	27.1344	27.2373	0.1029
				-**C**OOH	179.8104	179.8243	0.0139
β-CD				*β*-CD			
H-1	5.1163	5.1087	-0.0076	C-1	101.7985	101.8117	0.0132
H-2	3.6987	3.6959	-0.0028	C-2	71.7439	71.7756	0.0317
H-3	4.0118	3.9902	-0.0216	C-3	73.0071	73.0794	0.0723
H-4	3.6303	3.6236	-0.0067	C-4	81.0657	81.0378	0.0279
H-5	3.9235	3.9176	-0.0059	C-5	72.0102	72.0339	0.0237
H-$6_{a,b}$	3.9033	3.8837	-0.0196	C-6	60.2042	60.1932	-0.0110

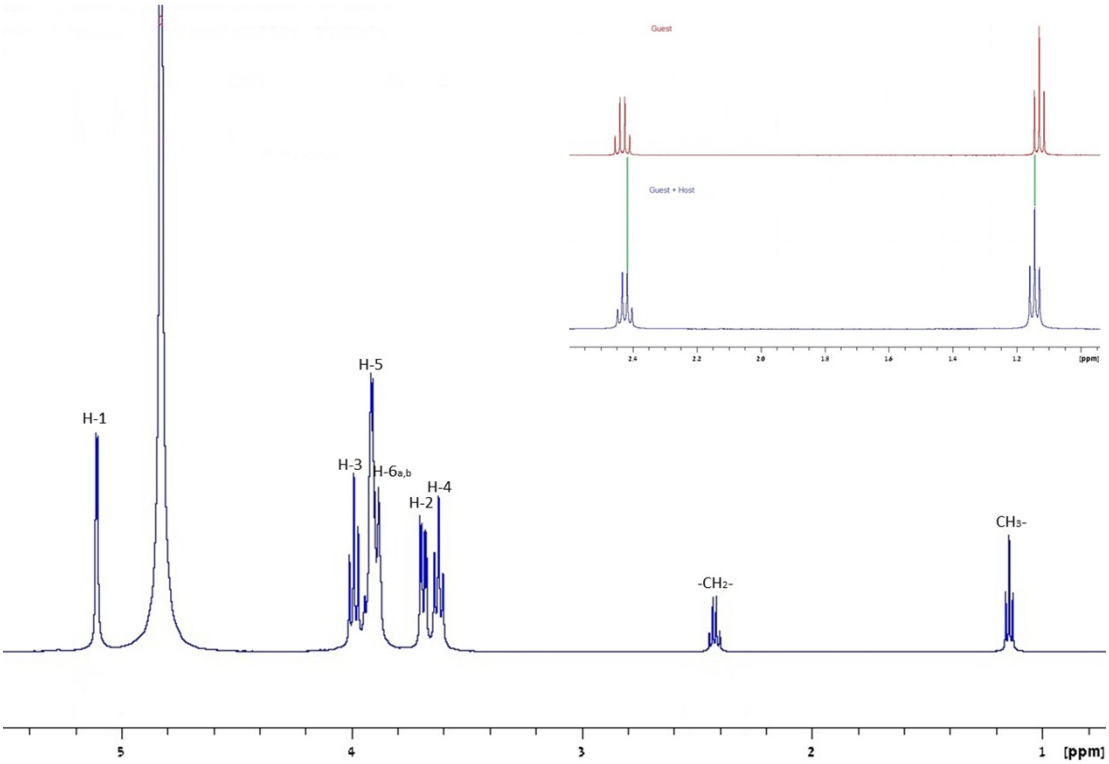

Figure S1 ^{1}H-NMR of *β*-CD-PA, 500 MHz in D_2O at 298º K. Enlarged are PA's methyl and methylene protons in free form (*Guest*) and in *β*-CD-PA inclusion complex form.

Table S2 Diffusion Coefficients *D* [X10^{5}cm^{2}s^{-1}] for PA, *β*-CD and *β*-CD-PA, corrected values (*X*), computed association constant *Ka* [M^{-1}] and *ΔG* [kJmol^{-1}].

Substance	*D* (D_2O)	*D* (host)	*D* (guest)	*X*
PA	1.6813±0.0025		0.7664±0.0017	0.7664±0.0017
β-CD	1.6410±0.0010	0.2217±0.0005		0.2271±0.0005
β-CD-PA	1.6316±0.0025	0.2199±0.0004	0.7059±0.0018	0.2266±0.0004 0.7274±0.0018
K_a	5.4502			
ΔG^o	-4.2011			

* As the diffusion coefficient of D_2O in the host/guest solution was different from the value obtained in the solution containing the host in the free state, the ratios of the two values were used to correct the experimental values giving rise the corrected values in the *X* column.

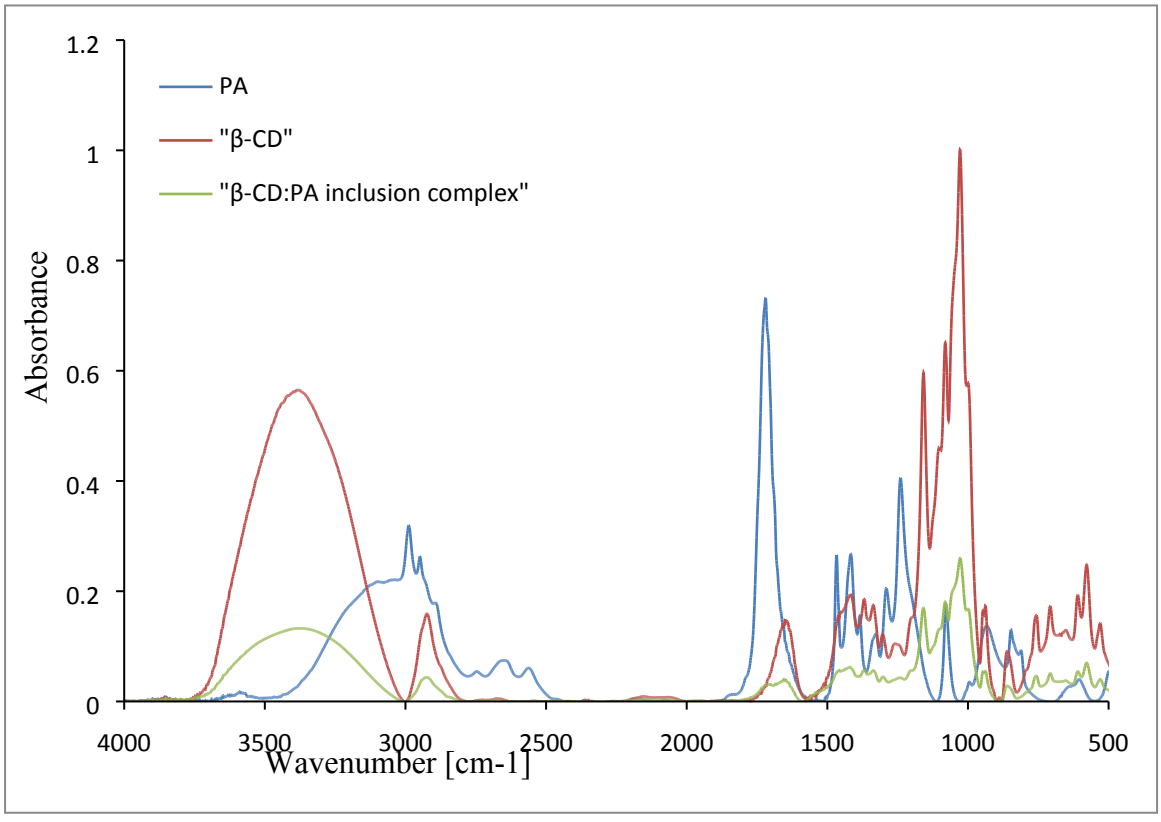

Figure S2 FTIR scan of *β*-CD (blue), PA (red) and *β*-CD-PA inclusion complex (green).

Thermodynamic Data

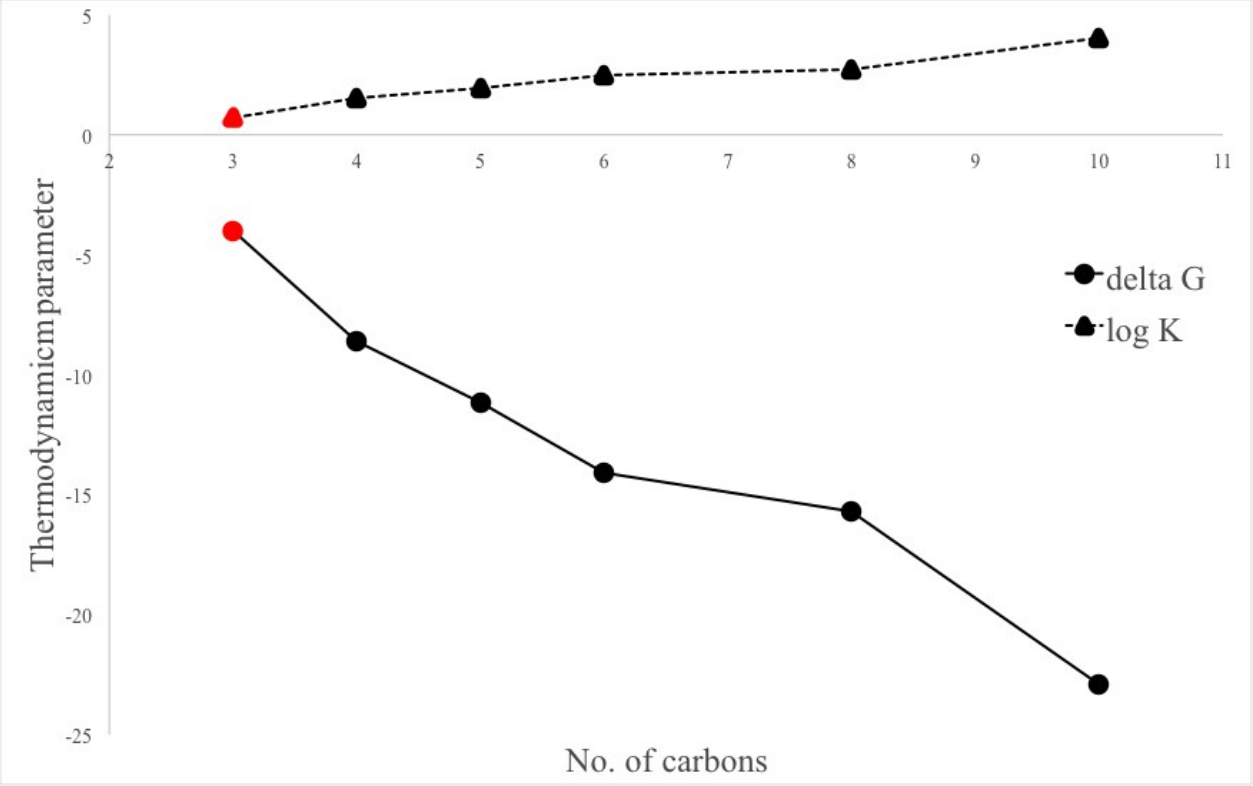

Figure S3 Rekharsky's plot of thermodynamic parameters vs. the number of carbons in several short fatty acids in their respective *β*-CD ICs. Our results successfully align this trend at 3 carbons for PA (red).

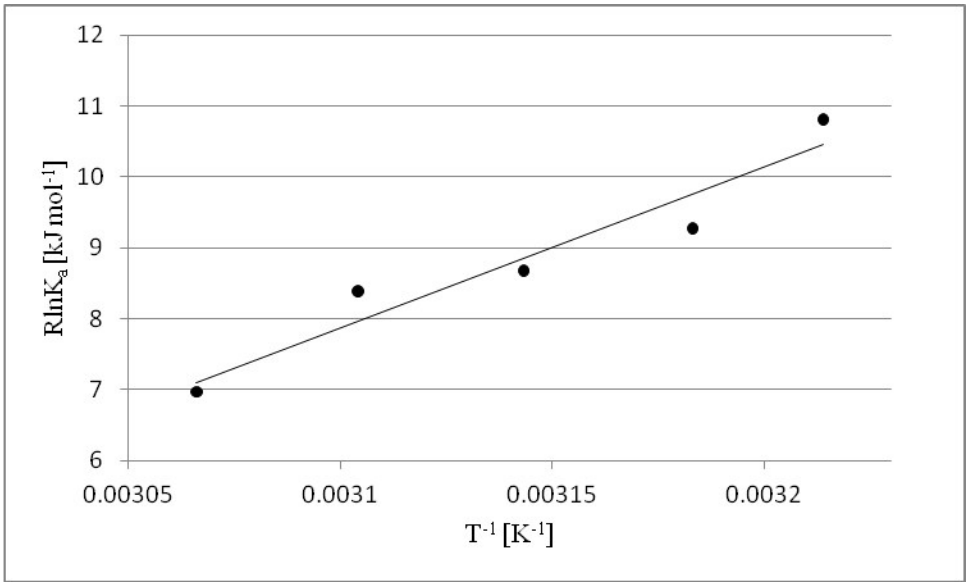

Figure S4 Van't Hoff plot for the *β*-CD-PA association.

Table S3 Temperature dependence of the apparent binding constant K_a between β-CD and PA as well as calculated enthalpy, entropy (at 298º K), Gibbs free energy and association constant (at 298º K) calculated from the linear relationship between $RlnK_a$ and T^{-1} by using the Van't Hoff equation.

$K_{a,298}$ [M^{-1}]	ΔG^o [$kJmol^{-1}$]	$T\Delta S^o$ [$kJmol^{-1}$]	ΔH^o [$kJmol^{-1}$]	K_a [M^{-1}]	T [K]
5.2±0.3	-4.1±0.1	-18.6±0.3	-22.7±0.7	3.5±0.3	311±1
				3.3±0.3	314±1
				2.9±0.3	318±1
				2.6±0.2	322±1
				2.4±0.2	326±1

Crystallographic Data

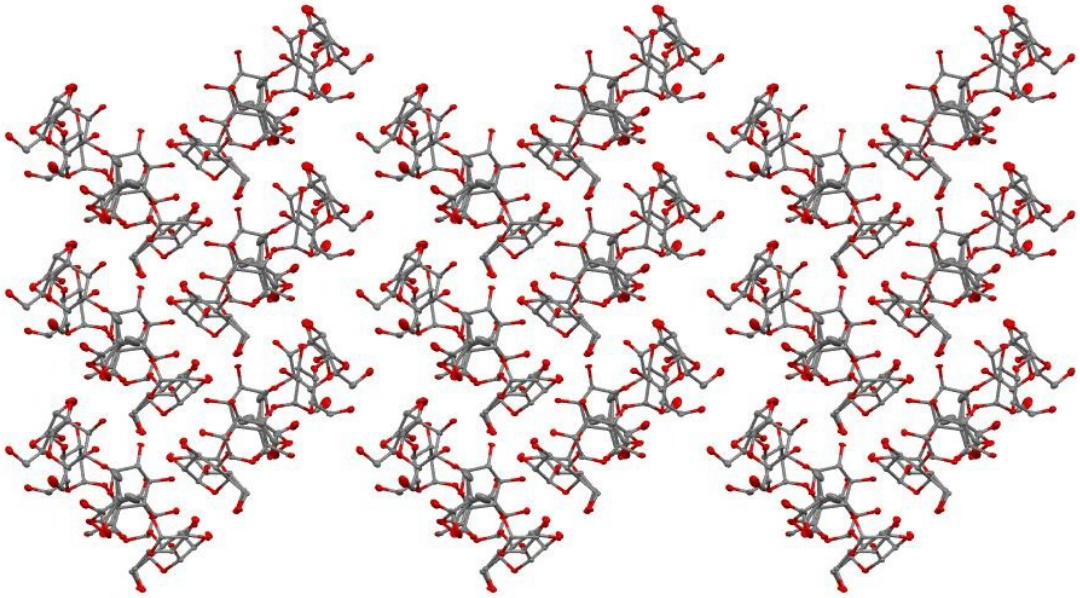

Figure S5 Herringbone-type packing of the PA-*β*-CD inclusion complexes.

Table S4 Crystal data and structure refinement for the PA-*β*-CD inclusion complex.

Empirical formula	$C_{90}H_{187}O_{100}$
Chemical formula moiety	$2(C_{42}H_{70}O_{35})$, $2(C_3H_6O_2)$, $26(H_2O)$
Formula weight	2869.40
Temperature	100(2) K
Diffractometer	Bruker KappaApexII CCD
Wavelength	0.71073 Å
Crystal system, space group	monoclinic, $P2_1$
Unit cell dimensions	a = 15.517(3) Å b = 9.825(2) Å beta = 90.05(3)^o c = 21.953(4) Å
Volume	3346.8(11) Å^3
Z, Calculated density	1, 1.424 Mg/m^3
Absorption coefficient	0.132 mm^{-1}
F(000)	1527
Crystal size	0.18 x 0.15 x 0.06 mm
θ range for data collection	2.62 to 25.68 deg
Limiting indices	-18<=h<=18, -11<=k<=11, -26<=l<=24
Reflections collected / unique	35149 / 12402 [R_{int} = 0.0820]
Completeness to θ = 25.68^o	99.8 %
Max. and min. transmission	0.9922 and 0.9767
Refinement method	Full-matrix least-squares on F^2
Data / restraints / parameters	12402 / 64 / 1015
Goodness-of-fit on F^2	1.052

Final R indices [I>2σ(I)]	R1 = 0.0669, wR2 = 0.1716
R indices (all data)	R1 = 0.0729, wR2 = 0.1768
Largest diff. peak and hole	0.694 and -0.462 e/Å^3

Table S5 Selected bond distances [Å] and angles [^{o}].

O1 - C64	1.428(7)
O1 - C1	1.428(6)
O2 - C2	1.427(7)
O3 - C3	1.436(6)
O4 - C6	1.444(7)
O5 - C1	1.414(6)
O5 - C5	1.430(7)
O11 - C11	1.405(7)
O11 - C4	1.428(7)
O12 - C12	1.417(7)
O13 - C13	1.414(6)
O14 - C16	1.416(7)
O15 - C11	1.420(6)
O15 - C15	1.440(6)
O21 - C21	1.410(6)
O21 - C14	1.429(6)
O22 - C22	1.419(7)
O23 - C23	1.414(7)
O24 - C26	1.434(7)
O25 - C21	1.412(6)
O25 - C25	1.440(7)
O31 - C31	1.415(7)
O31 - C24	1.443(6)
O32 - C32	1.406(7)
O33 - C33	1.429(7)
O34 - C36	1.418(8)
O35 - C31	1.419(7)
O35 - C35	1.433(8)
O41 - C41	1.412(7)
O41 - C34	1.424(7)
O42 - C42	1.423(8)
O43 - C43	1.457(8)
O44 - C46	1.423(8)
O45 - C41	1.409(7)
O45 - C45	1.429(7)
O51 - C51	1.411(7)
O51 - C44	1.431(7)
O52 - C52	1.415(7)
O53 - C53	1.417(7)
O54 - C56	1.411(11)

O55 - C51	1.405(8)
O55 - C55	1.440(8)
O61 - C61	1.411(6)
O61 - C54	1.441(7)
O62 - C62	1.436(7)
O63 - C63	1.415(7)
O64 - C66	1.442(7)
O65 - C61	1.418(7)
O65 - C65	1.437(6)
C1 - C2	1.521(8)
C2 - C3	1.522(7)
C3 - C4	1.523(7)
C4 - C5	1.529(7)
C5 - C6	1.510(7)
C11 - C12	1.532(8)
C12 - C13	1.530(7)
C13 - C14	1.540(7)
C14 - C15	1.521(8)
C21 - C22	1.522(8)
C22 - C23	1.526(8)
C23 - C24	1.526(7)
C24 - C25	1.543(7)
C25 - C26	1.514(7)
C31 - C32	1.538(8)
C32 - C33	1.522(8)
C33 - C34	1.509(8)
C34 - C35	1.525(8)
C35 - C36	1.519(8)
C41 - C42	1.538(9)
C42 - C43	1.502(9)
C43 - C44	1.518(8)
C44 - C45	1.542(8)
C45 - C46	1.509(8)
C51 - C52	1.528(8)
C52 - C53	1.517(8)
C53 - C54	1.510(8)
C54 - C55	1.532(8)
C55 - C56	1.505(9)
C61 - C62	1.520(8)
C62 - C63	1.524(8)
C63 - C64	1.528(7)
C64 - C65	1.526(7)
O3 – O14	2.849(6)
O3 – H14	2.01
O4 – O12	2.764(6)
O4 – H12	1.93

O13 – O63 2.748(6)
O13 – H63 1.91
O14 – O36 2.683(7)
O22 – O8 2.706(10)
O22 - O10 2.790(12)
O23 – O9 2.949 (12)
O23 – O36 2.741(6)
O24 – O16 2.699(6)
O32 – O16 2.677(6)
O32 – O36 2.660(6)
O34 – O38 2.71(3)
O44 – O17 2.719(8)
O44 – O19 2.747(10)
O52 – O26 2.781(6)
O53 – O16 2.774(6)
O54 – O30 2.698(8)
O62 – O37 2.749(6)
O64 – O37 2.763(6)
O6 - C7 1.22(2)
O7 - C7 1.262(17)
C7 - C8 1.50(3)
C8 - C9 1.54(2)
O6 - C7 - O7 126.6(17)
O6 - C7 - C8 121.8(17)
O7 - C7 - C8 111.5(14)
C7 - C8 - C9 109.4(18)
O6A - C7A 1.26(3)
O7A - C7A 1.29(4)
C7A - C8A 1.50(4)
C8A - C9A 1.53(5)
O6A - C7A - O7A 124(2)
O6A - C7A - C8A 121(2)
O7A - C7A - C8A 114(3)
C7A - C8A - C9A 112(3)
O6 – C6 3.420(18)
O6 – H6B 2.873
O6 – C15 3.564(18)
O6 – H15 2.692
O7 – C25 3.515(9)
O7 – H25 2.630
O7 – C36 3.368(9)
O7 – H36C 2.819
O7 – C35 3.455(9)
O7 – H35 2.788
O6A – H17B 2.02(9)
O7A – C15 3.50(3)

O7A – H15	2.678
O42 – O7	2.736(8)
O43 – O6	2.679(18)
H43 – O6	1.98
O43 – O7A	2.71(3)

Computational Data

Visual representations of *β*-CD-PA inclusion complex configurations

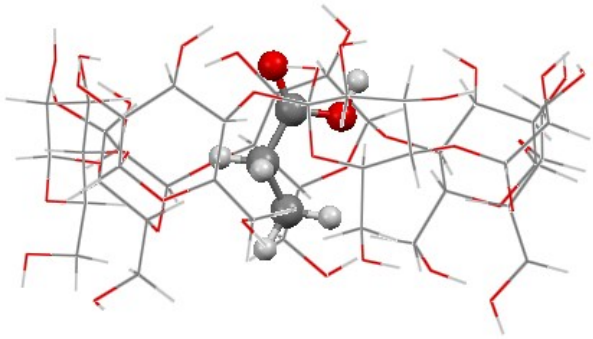

Figure S6 Neutral PA, fully immersed, O-2, O-3 side

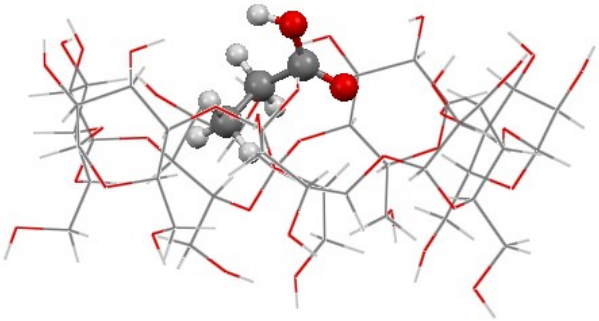

Figure S7 Neutral PA, partially immersed, O-2, O-3 side

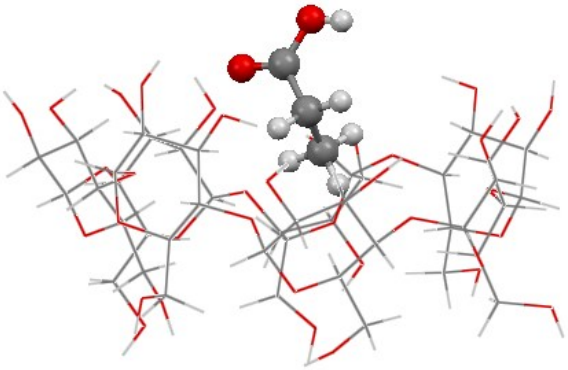

Figure S8 Neutral PA, partially unbound, O-2, O-3 side

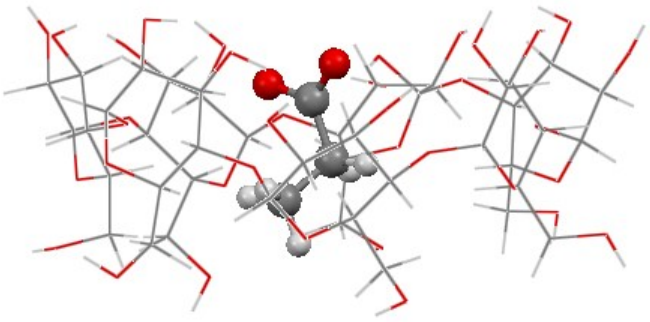

Figure S9 Anionic, fully immersed, O-2, O-3 side

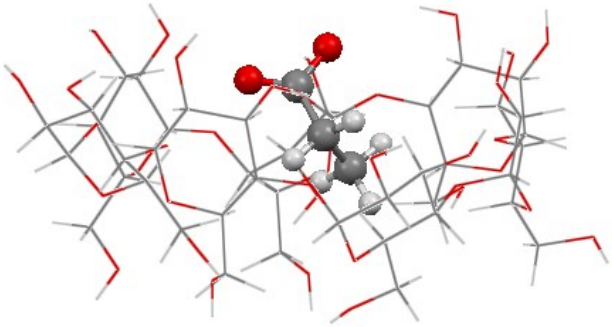

Figure S10 Anionic, partially immersed, O-2, O-3 side

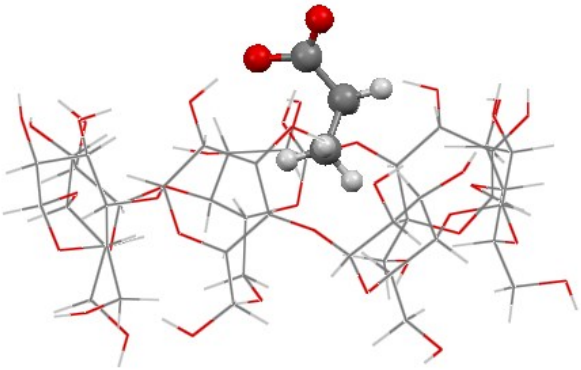

Figure S11 Anionic, partially unbound, O-2, O-3 side

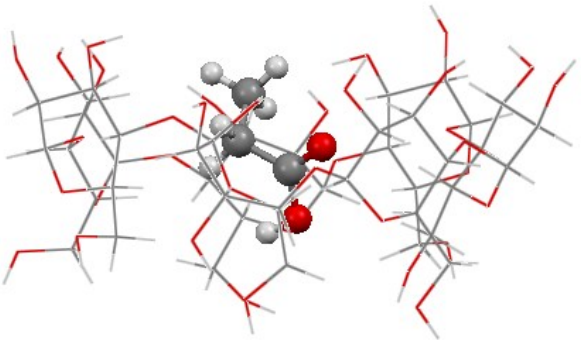

Figure S12 Neutral PA, fully immersed, O-6 side

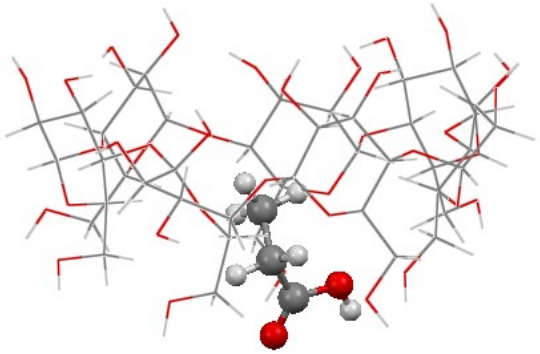

Figure S13 Neutral PA, partially immersed, O-6 side

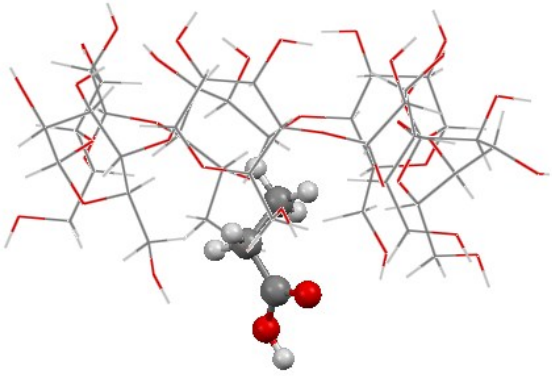

Figure S14 Neutral PA, partially unbound, O-6 side

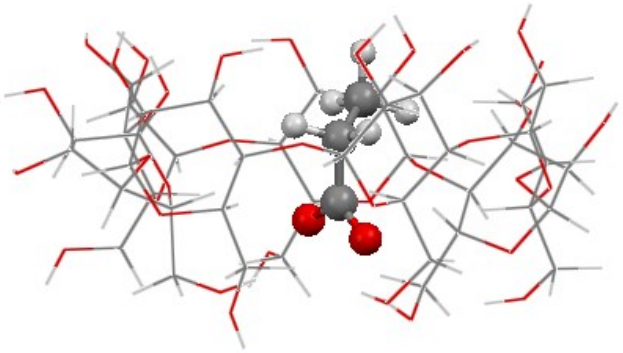

Figure S15 Anionic, fully immersed, O-6 side

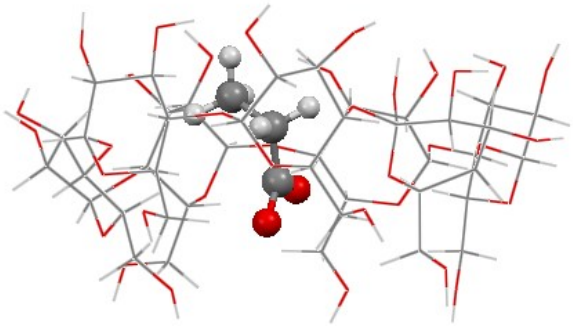

Figure S16 Anionic, partially immersed, O-6 side

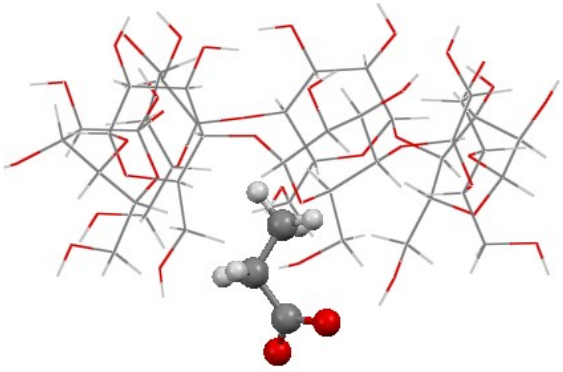

Figure S17 Anionic, partially unbound, O-6 side

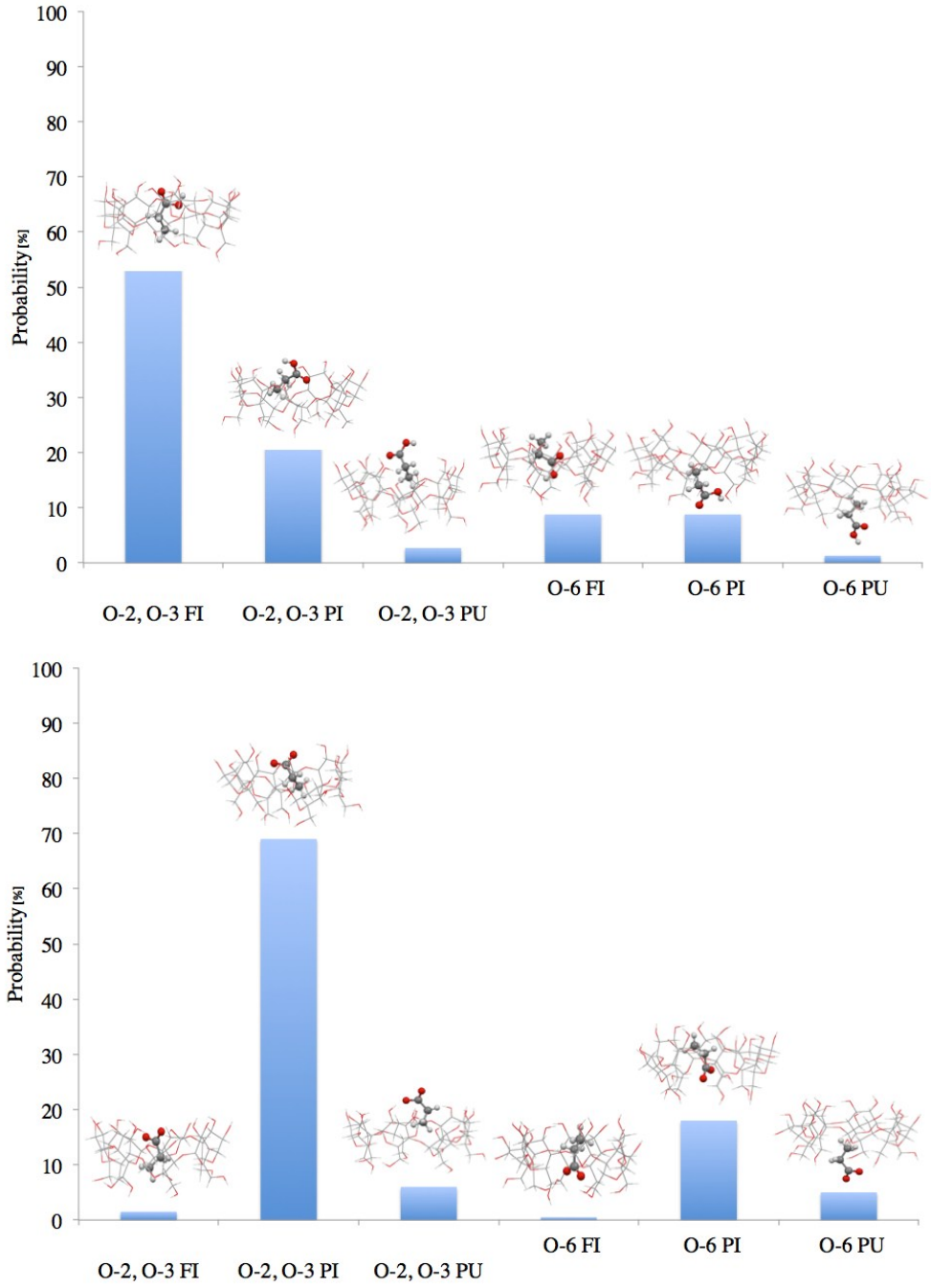

Figure S18 Probability dispersion for the different computed configurations. (top) neutral PA, (bottom) anionic PA, FI fully immersed, PI partially immersed, PU partially unbound. PA's anionic form was also simulated. Importantly, analysis of the MD trajectories showed that in comparison to the neutral form, the anionic form is less tightly bound to β-CD. It shows a higher mobility and fast motion between the β-CD cavity and the bulk solvent. Thus, PA's anionic form led to a less stable IC than its neutral form. These results are in correlation with previous works that mentioned that an electrical charge on the guest acid's carboxyl head has a considerable effect on the kinetic characteristics of the complexation reaction.[16,17] In contrast to neutral PA,

the anionic form moved rapidly toward the water solvent after 2 ns of simulation. During this process, the anionic form was found to sometimes visit the "fully immersed" and "partially unbound" states. The "partially immersed" configuration was found to be dominant for PA's anionic form.

Table S6 Probability statistics for computed configurations of PA-*β*-CD.

form PA	Configuration	Probability]%[	
		O-2, O-3 orientation	O-6 orientation
neutral[a]	fully immersed	55	9
	immersed partially	21	9
	unbound partially	2.7	1.3
anionic	fully immersed	1.5	0.5
	immersed partially	69	18
	partially unbound	6	5

[a] Neutral PA's probabilities do not sum up to 100% since 'fully unbound' configurations were observed as well by a low total probability of 2%.

Table S7 Frequency of neutral PA-Water and PA-*β*-CD contacts/encounters (per 1 ps time step unit) estimated from MD trajectories for each structural PA fragment. System/mixture 1-3 (see Methods).

Main period, 10-50 ns (after eq.)		Initial period, first 5 ns (eq. step)		PER structural fragments
β-CD (OH)	H_2O	*β*-CD (OH, C, O)	H_2O	
				Total
1.37 (OH)	0.95	1.8 (OH)	1.1[a]	PA_O1H
0.6 (OH)	1.44	0.7 (OH)	0.32[a]	PA_O2
2.0 (OH)	2.4	2.5 (OH)	1.42[a]	-COOH
5.1 (OH)	0.24	4.1 (OH)	0.35	Alkyls

[a] frequency of hydrogen bonding and VDW contact events.

Table S8 Frequency of anionic PA-Water and PA-*β*-CD contacts/encounters (per 1 ps time step unit) estimated from MD trajectories for each structural PA fragment. System/mixture 1-2 (see Methods).

Main period, 10-50 ns (after eq.)		Initial period, first 5 ns (eq. step)		PER structural fragments
β-CD (OH)	H_2O	*β*-CD (OH, C, O)	H_2O	
				Total
0.71 (OH)	1.45	1.5 (OH)	0.81[a]	PA_O1
0.8 (OH)	1.6	0.8 (OH)	0.45[a]	PA_O2
1.5 (OH)	3.1	2.3 (OH)	1.30[a]	$-COO^-$
3.9	0.24	4.5 (C, O)	0.19	Alkyls

[a] frequency of hydrogen bonding and VDW contact events.

a 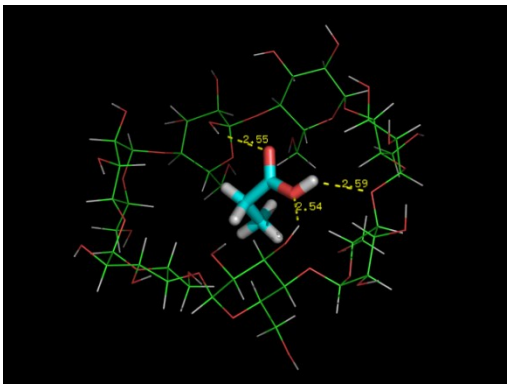 b 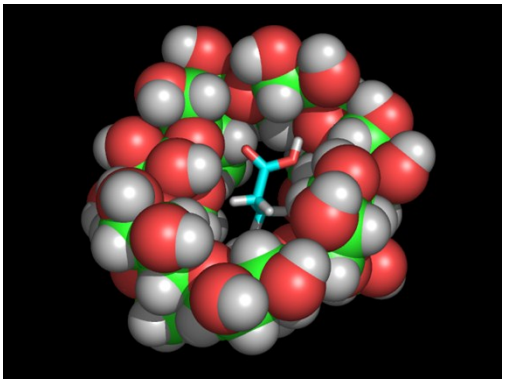

Figure S19 hydrogen bond (a) and VDW (b) interactions in the *β*-CD-PA (neutral form) IC in its fully immersed configuration. The IC "visits" this state approximately ~64% of the MD simulation time. PA molecules usually form 2 or 3 weak hydrogen bonds with *β*-CD's oxygen atoms (less frequent event). The figure shows two hydrogen-bonds between PA's protonated oxygen and *β*-CD oxygen atoms. A third hydrogen bond is formed between PA's non-protonated carbonyl oxygen and a *β*-CD hydroxyl. Interestingly, this proton free carbonyl oxygen is still accessible to water molecules, but at this moment of our MD trajectory representation there are no hydrogen bonds between PA and water. Another interesting observation is PA-induced changes in the conformational dynamics of the *β*-CD molecule. One edge of the *β*-CD cone is "shrinking" due to interaction with PA's alkyl moiety.

References

1 E. O. Stejskal, J. E. Tanner, *J. Chem. Phys.* **1965**, *42,* 288. For a review on the applications of the PGSE NMR technique to chemical systems, see: P. Stilbs, *Prog. NMR Spectrosc*. 1987, **19***,* 1 and references therein.

2 a) O. Mayzel, Y. Cohen, *J. Chem. Soc., Chem. Commun.* 1994, 1901; b) O. Mayzel, O. Aleksiuk, F. Grynszpan, S. E. Biali, Y. Cohen, *J. Chem. Soc., Chem. Commun.* 1995, 1183; c) A. Gafni, Y. Cohen, *J. Org. Chem.* 1997, **62**, 120; d) O. Mayzel, A. Gafni, Y. Cohen, *Chem. Commun.* 1996, 911; e) L. Frish, S. E. Matthews, V. Böhmer Y. Cohen, *J. Chem. Soc., Perkin Trans.* 1999, **2**, 669; f) A. Gafni, Y. Cohen, R. Kataky, S. Palmer, D. Parker, *J. Chem. Soc., Perkin Trans.* 1998, **2**, 19; g) Y. Cohen, L. Avram, L. Frish, *Angew. Chem. Intr. Ed.*, 2005, **44**, 520.

3 L. Frish, F. Sansone, A. Casanti, R. Ungaro, Y. Cohen, *J. Org. Chem.* 2000, **65,** 5026.

4 R. Wimmer, F. L. Aachmann, K. L. Larsen, S. B. Petersen, *Carbohydr. Res*. 2002, **337**, 841.

5 I. R. Gelb, L. M. Schwartz, B. Cardelino, H. S. Fuhrman, R. F. Johnson, D. A. Laufer, *J. Am. Chem. Soc.* 1981, **103,** 1750.

6 I. J. Lee, G. S. Jung, K. Kim, *J. Solution Chem*. 1994, **23,** 1283.

7 A. Lutka, B. Golda, *Acta Pol. Pharm.* 2006**, 63**, 3.

8 R. W. Harrison, *J. Comp. Chem.* 1993, **14**, 1112.

9 H. J. C. Berendsen, D. Van-Der-Spoel, R. Vandrunen, *Comput. Phys. Commun.* 1995, **91**, 43.

10 E. Lindahl, B. Hess, D. Van-Der-Spoel, *J. Mol. Model.* 2001, **7**, 306.

11 A. K. Malde, L. Zuo, M. Breeze, M. Stroet, D. Poger, P. C. Nair, C. Ostenbrink, A. E. Mark, *Chem. Theory Comput.* 2011, **7**, 4026.

12 B. Hess, H. Bekker, H. J. C. Berendsen, J. G. E. M. Fraaije, *J. Comput. Chem.* 1997, **18,** 1463.

13 T. Darden, D.York, L. Pedersen, *J. Chem. Phys.* 1993, **98**, 10089.

14 U. Essmann, L. Perera, M. L. Berkowitz, T. Darden, H. Lee, L. G. Pedersen, *J. Chem. Phys.* 1995, **103**, 8577.

15 H. J. C. Berendsen, J. P. M. Postma, W. F. Vangunsteren, A. Dinola, J. R. Haak, *J. Chem. Phys.* 1984, **81**, 3684.

16 S. Nishikawa, M. Kondo, *J. Phys. Chem. B.* 2006, **110**, 26143.

17 J. R. Bae, *J. Korean. Phys. Soc.* 2013, **63**, 193.